Continuous Molecular Monitoring of Human Dermal Interstitial Fluid with Microneedle-Enabled Electrochemical Aptamer Sensors.

Mark Friedel,*[a] Benjamin Werbovetz, [a] Amy Drexelius,[a] Kevin W. Plaxco[b], and Jason Heikenfeld[a]

The ability to continually collect diagnostic information from the body during daily activity has revolutionized the monitoring of health and disease. Much of this monitoring, however, has been of physical "vital signs," with the monitoring of molecular markers having been limited to glucose, primarily due to the lack of other medically relevant molecules for which continuous measurements are possible in bodily fluids. Electrochemical aptamer sensors, however, have a recent history of successful in-vivo demonstrations in rat animal models. Herein, we present the first report of real-time human molecular data collected using such sensors, successfully demonstrating their ability to measure the concentration of phenylalanine in dermal interstitial fluid after an oral bolus. To achieve this, we used a device that employs three hollow microneedles to couple interstitial fluid to an ex-vivo, phenylalanine-detecting sensor. The resulting architecture achieves good precision over the physiological concentration range and clinically relevant, 20 min time lag times. By also demonstrating 90 day dry room-temperature shelf-storage, the reported work also reaches another important milestone in moving such sensors to the clinic. While the devices demonstrated are not without remaining challenges, the results at minimum provide a simple method by which aptamer sensors can be quickly moved into human subjects testing.

Introduction

Wearable devices supporting the continuous monitoring of glucose in dermal-interstitial fluid have transformed the management of diabetes. This singular, but major, success in the high-frequency measurement of a molecular biomarker[1] has inspired broader pursuit of biosensors supporting similarly real-time, high-frequency measurements of markers indicative of the numerous other disease and health conditions that could benefit from continuous monitoring.

A challenge to expanding continuous molecular monitoring beyond glucose is access to a biofluid containing meaningful concentrations of the analyte of interest. Blood is the most well characterized and well understood biofluid, but its continuous access is invasive. Many other biofluids, including tears, saliva, sweat, and urine, can be collected non- or minimally-invasively. These, however, are cumbersome or impossible to collect continuously and often fail to accurately reflect the analyte concentrations found in blood[1,2]. The remaining biofluid option, interstitial fluid (ISF), is easily accessed in the dermis, as this tissue lies less than a millimetre beneath the skin surface. Dermal ISF is rich in biomolecules; it contains >90% of the proteins, RNAs, and metabolites found in blood, as well molecules unique to the ISF[3–5]. A wide-ranging array of methods exist for access of dermal ISF[6] including direct insertion of needle-based electrochemical sensor similar to those used in continuous glucose meters.

While ISF has significant promise for the measurement of analytes beyond glucose, a second challenge has been the generation of sensors that, unlike the enzymatic sensors used in glucose monitors, are independent of the chemical reactivity of their targets. That is, due to the modest number of oxidoreductive or other "sensor-ready" enzymes, enzyme-based sensing approaches are not easily generalizable to most of the analytes accessible in ISF. Finding new sensing modalities has proven challenging, as any alternative to enzymatic sensors should maintain their many advantages, including their high measurement frequency and their ability to operate without the addition of exogenous reagents. Electrochemical aptamer-based (EAB) sensors, however, achieve these attributes while also relying on target binding rather than the chemical transformation of their target, rendering them as generalizable as the aptamers they employ for target recognition. And given that aptamer libraries start with trillions of randomly generated, potential aptamers[7,8] which can then be further chemically modified to enhance their binding and tune it to in-vivo detection needs, the generalizability of aptamers appears broad[9].

wire and introduced using an intravenous catheter[10,11]; only limited examples have been reported in which, as is true for continuous glucose monitors[12], such devices have been adapted to microneedles suitable for performing measurements in the

[a] *Novel Devices Laboratory, Department of Biomedical Engineering, University of Cincinnati, Cincinnati, Ohio 45221, USA*
[b] *Department of Chemistry and Biochemistry, University of California, Santa Barbara, Santa Barbara, CA 93106*
[c] ** Send correspondence to: Mark Friedel: friedemc@mail.uc.edu*
Electronic Supplementary Information (ESI) available: 2D AutoCAD files for device parts & shadow mask are provided. Additional sensor data is also available

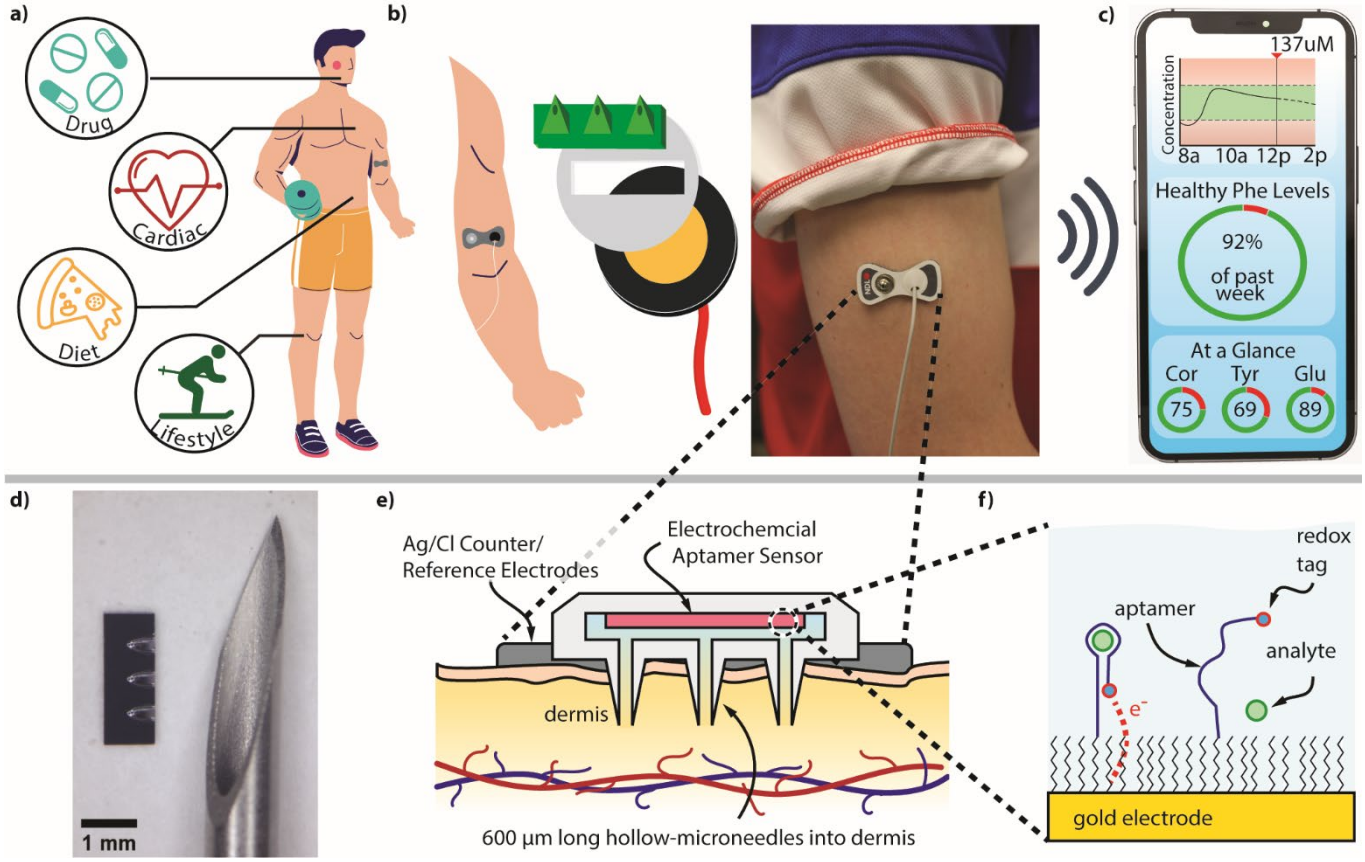

Figure 1 - Schematics, images, and illustrations of wearable aptamer sensors for continuous molecular monitoring of the dermal ISF. **a.** Potential application spaces for continuous, wearable aptamer sensors ranging from clinical cardiac or therapeutic drug monitoring to metabolic and health related consumer products. **b.** Visualization of device components and an image of the on-body device. **c.** A mock-up of a mobile application supporting continuous, aptamer-based sensing devices. **d.** Comparison of the 3x1 microneedle array with a standard, 18-gauge needle of the type commonly used in blood donation. **e.** A schematic of our microneedle device on-body with **f.** a schematic of the sensor mechanism[7].

dermis[13]. And while these demonstrations represent a significant advance in in vivo molecular monitoring, all prior reports have been limited to rats, the overwhelming majority of which were anesthetized during study. It is unclear how well such devices function in ambulatory animal studies, and even more uncertain in human subjects as no human data has been reported thus far.

A challenge associated with moving to human subjects is that the device requirements are much more stringent than for animals. For example, for human use an ideal device should be minimally invasive and allow for safe and easy insertion, wear, and removal. In support of this, and to increase design freedom, here we have employed ex-vivo sensors coupled to the dermis via FDA-approved, hollow microneedles (Figure 1b) that, because they penetrate less than 700 µm, are generally painless and avoid bleeding. This design also only introduces one foreign material, silicon, directly to the body, lowering the risk for immune response or unwanted materials leeching into the body. Finally, the ex-vivo placement of the sensors in this design also allows for additional "modules," such as a protective membrane or components supporting preconcentration of the analyte[14,15], to control the sensing environment in ways that cannot be achieved with indwelling sensor.

Leveraging these hollow microneedles, herein we report the first on-body, human dose-response data derived using an EAB sensor. In achieving this, the first in-human data for any type of continuous, affinity-based biosensor, our work has surmounted a number of key milestones in the practical, continuous molecular monitoring of analytes beyond glucose. First, the work presented demonstrates practical tools for the manufacturing and dry-shelf storage of devices employing electrochemical aptamer-based sensors. Second, we demonstrate the utility of employing simple, gel-pad skin adhesive counter and reference electrodes, which simplify device construction and testing[16]. Finally, our design reduces the skin damage of previous (enzymatic sensor) in-vivo microneedle demonstrations, which required 10s to 100s of perforations[12,17], by employing only 3.

Results & Discussion

Device Structure and Function

Our device is a low profile, minimally-invasive, wearable design in which the sensor remains ex-vivo and only FDA approved microneedles (from Nanopass Tech. Ltd.) enter the body (Figure 1). These hollow, fluid-filled microneedles create a coupling that

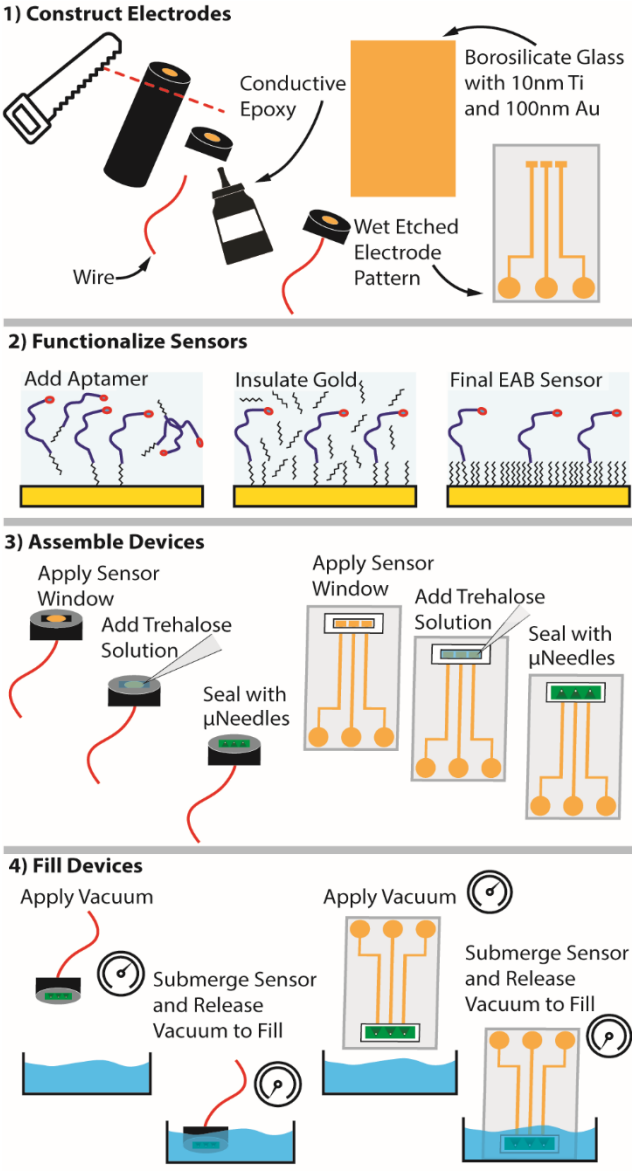

Figure 2 - Device Fabrication. Shown is the fabrication process employed for both the disc (left) and custom planar (right) gold electrode devices.

allows the analyte to rapidly diffuse to the sensor. This coupling also acts as a failsafe for immediate detection of failed insertions; without the fluidic connection between the sensor and the dermis the device does not pass measurable currents. The device is relatively simple to construct: a gold working electrode modified with the target-recognizing aptamer is sealed against the microneedles (figure 1b) and then surrounded by a gel Ag/AgCl counter electrode that covers the surrounding skin surface. The fabricated device is placed onto the arm and gentle pressure is applied by hand to ensure microneedle penetration (no specialized "inserter" is required). In this work, we attached the electrodes to a bench-top potentiostat, and then employed square wave voltammetry to interrogate the sensor. With the addition of a miniaturized potentiostats[16], this approach could readily be adapted to a fully self-contained, wearable device supporting continuous, real-time molecular monitoring (figure 1a & c).

Simulation Results

Simulations of the time required to reach 90% of the "dermal" (i.e., applied) analyte concentration at the sensor surface suggest that, for low molecular weight (<3 kDa) analytes, the lag times associated with our ex-vivo sensor placement would be on the order of tens of minutes (Figure 3a & b). To perform these simulations, we construct a model dermis, microneedle lumen, and sensor space and set a homogenous concentration throughout the entire model (figure 3b). Then we spike simulated dermis with 5 mM of the target and monitor the concentration seen at the furthest point from the microneedle lumen. Doing so we found that, with glucose (180 Da) as the target, the sensor surface reaches 90% of its final concentration within 20 min, a time scale that compares well with the previously demonstrated 11 min lag times of a similar, on-body, microneedle-based continuous glucose monitor[17]. Using the amino acid phenylalanine (165 Da) as the target this lag time decreases to 17 min, and for the antibiotic vancomycin (1449 Da) times it increases to 50 min. Not surprisingly, our device performs more poorly for higher molecular weight analytes. For inflammatory marker IL-6 (21 kDa), for example, the concentration at the distal site reaches only 31% of the dermal analyte concentration even after 2h.

Sensor fabrication and preservation

Before use, we must prime our devices to create the required fluidic connection between the ISF and our sensors. Due to the hydrophobic nature of the needle lumen, we employ vacuum to perform this priming. Unfortunately, however, electrochemical aptamer sensors lose functionality after exposure to vacuum (figure 4b). We speculate that this is due to physical desorption of the sensor surface chemistries, removing both aptamers and portions of the mercaptohexanol monolayer. To circumvent this, we deposited 10% trehalose solution onto the sensing surface and dry the sensors under vacuum, an approach similar to those often used to preserve DNA[18]. Such treatment not only preserves the aptamer, but also impedes desorption of the gold-thiol bonds at the sensor surface (figure 4c). Critically, phenylalanine-detecting sensors dried in trehalose solution under vacuum and later rehydrated respond to their target with the same affinity and gain as we observed before drying (figure 4d).

In addition to protecting sensors during priming, trehalose treatment also preserves sensors for dry, long-term, room temperature storage, an important consideration for clinical devices. To show this we tested trehalose preservation using two sensors: one targeting phenylalanine[10] and a second targeting cortisol[16]. We deposited trehalose solution on these sensors, dried them under vacuum, and stored them in dry nitrogen at room temperature for up to 90 days. After such storage, both sensors maintained their ability to respond to their targets after rehydrating in solution to remove the trehalose preservation layer (figure 4e & f). Specifically, at a square-wave frequency of 10 Hz, stored phenylalanine sensors exhibit signal gain (relative signal change at a given target

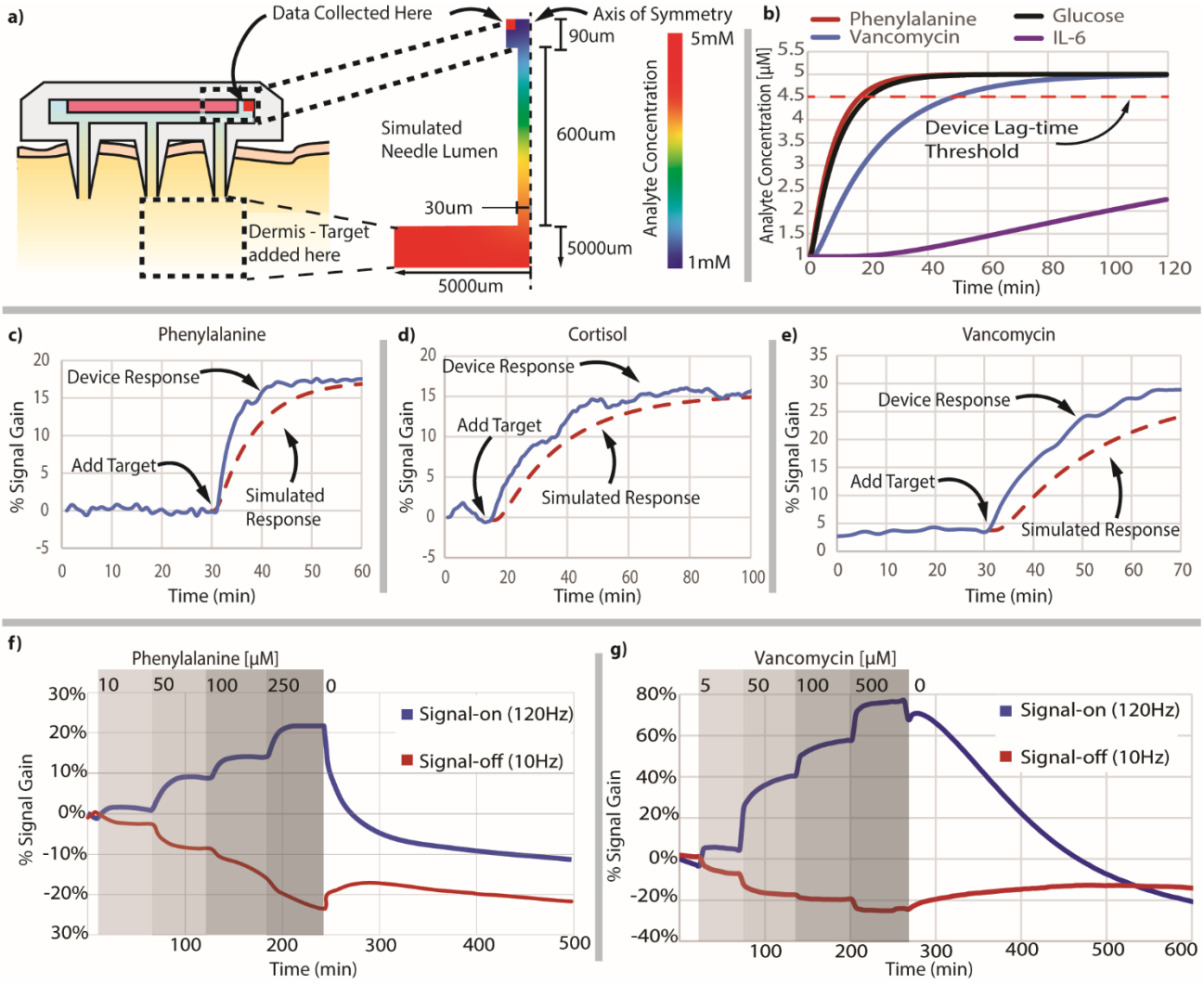

Figure 3 - Simulations and in-vitro device validation. a. Schematic of the device on-body compared to the representative geometry used in simulations. **b.** Simulated results for worst-case scenario measurements of multiple analytes in our sensing device. **c.** Comparison of in vitro device lag to simulated results on planar electrodes for phenylalanine, **d.** cortisol, and **e.** vancomycin. **f.** Titration of analyte to MN-EAB disc electrodes for phenylamine in PBS and **g.** vancomycin in a dilute serum as an ISF analogue.

concentration) within error of that seen in pre-storage controls. At higher frequencies (120 Hz for phenylalanine and 300 Hz for cortisol) the gain even increased slightly. This may be due to loss of non-specifically adsorbed aptamer, which would raise the background signal and thus reduce gain. Consistent with this, we see mild reductions in peak current after storage (figure 4g & h). This minor signal loss, is independent of the length of storage, furthering the argument it is not outright sensor degradation and suggests that dry storage under trehalose may be extendable to well beyond 90 days.

Device Design Effects on Signal Strength

In this work we have fabricated sensors using both commercial gold disc electrodes and custom, e-beam deposited, thin-film gold electrodes, both of which have advantages and disadvantages. Disc electrodes can be conveniently built using commercially available tools. Thin-film electrodes, in contrast, require more specialized tools to create but they enable the placement of the entire 3-electrode reference/counter/working system on a single, small chip. A second concern is that, even when the geometric surface area of the two is identical (3.14 mm^2) the peak currents associated with the thin-film electrodes are less than half those of the disk electrodes when they are free in solution (figure 4a). We believe this arises due to differences in the surface microstructure of the two electrode types. Disc electrodes, being reusable, are mechanically polished as part of preparation, which increases their roughness and thus their microscopic surface area. Consistent with this, cyclic voltammetry of the gold oxidation peak indicates that the electrochemically active surface area of disc electrodes is 49.5±0.3% larger than that of thin-film electrode of the same macroscopic dimensions (SI figure 1). Unfortunately, our attempts to increase the microscopic surface area of the thin-film electrodes via, for example mechanical polishing and electrochemical roughening[19], lead to poor reproducibility and increased sensor degradation (data not shown).

The peak currents of both disk and thin-film electrodes become poorer when these are integrated into microneedle devices. Specifically, the peak currents of sensors fabricated on disc electrodes decreased by 30% to 40% and those fabricated on

thin-film electrodes by 66% to 78% when these were integrated into microneedle devices. This may arise because the placement of electrodes in our microneedle devices limits the cross section of the solution available to pass current, which, which, when combined with the microneedle's acting as a capacitor, creates an RC circuit charging current. The stored charge in such a circuit cannot be measured, leading to lower current measurements.

Device Validation in vitro

Both thin-film and disc electrode devices achieve lag times of less than 30 min when we tested them in vitro (figure 3 c-e). Specifically, the lag times of our phenylalanine, cortisol, and vancomycin sensors (lag times as defined above) were 10, 29, and 28 min, respectively. This is more rapid than predicted by our simulations, presumably due to two factors: the compensatory, worst-case scenario simulation design and the assembly processes. For example, due to compression of the adhesive used to assemble our devices, the height of the sensing cavity is likely less than the 90 μm we designed, and smaller volumes will equilibrate more rapidly. Critically, given that clinical devices must work over a large range of target concentrations, we found similar diffusion lag times across all target concentrations (figure 3f & g). The diffusion of analyte out of our devices, however, is slower than the rate of diffusion into them. (I.e., the lag time for falling concentrations is greater than that of rising concentrations.) For example, when analyte concentration outside the device was lowered from 250 μM to 0 μM, our phenylalanine-detecting devices required ~64 min before it reported 90% of the final concentration change (figure 4f). Our vancomycin-detecting devices behaved similarly, requiring ~154 min to fall 90% when the applied concentration was lowered from 500 μM to 0 μM (figure 4g). We do not have empirical evidence suggesting a cause for this slow analyte elimination, but similar challenges have been seen in another diffusion-based, electrochemical aptamer device[14].

On-body Device Testing

Our microneedle-based devices support high-frequency molecular measurements on human subjects. To show this, we first fixed a phenylalanine-detecting devices onto a subject's arm and initiated data collection. After an initial set of measurements were collected, the subject was allowed to move and to complete light, everyday tasks while periodically returning to the potentiostat to perform further measurements over the course of 5 h. During this entire period, the sensor remained coupled to dermal ISF (figure 5a). While we performed these measurements the peak current decreased. This decrease is expected as it is seen regularly in in-vitro testing in serum, presumably as foulants diffuse to the sensing surface and reduce electron transfer.

The disc-electrode device detected the increase in ISF phenylalanine levels associated with an oral challenge (25 mg/kg) within 20 min, which then plateaued. This is consistent with the known physiology of phenylalanine, as previous, blood-

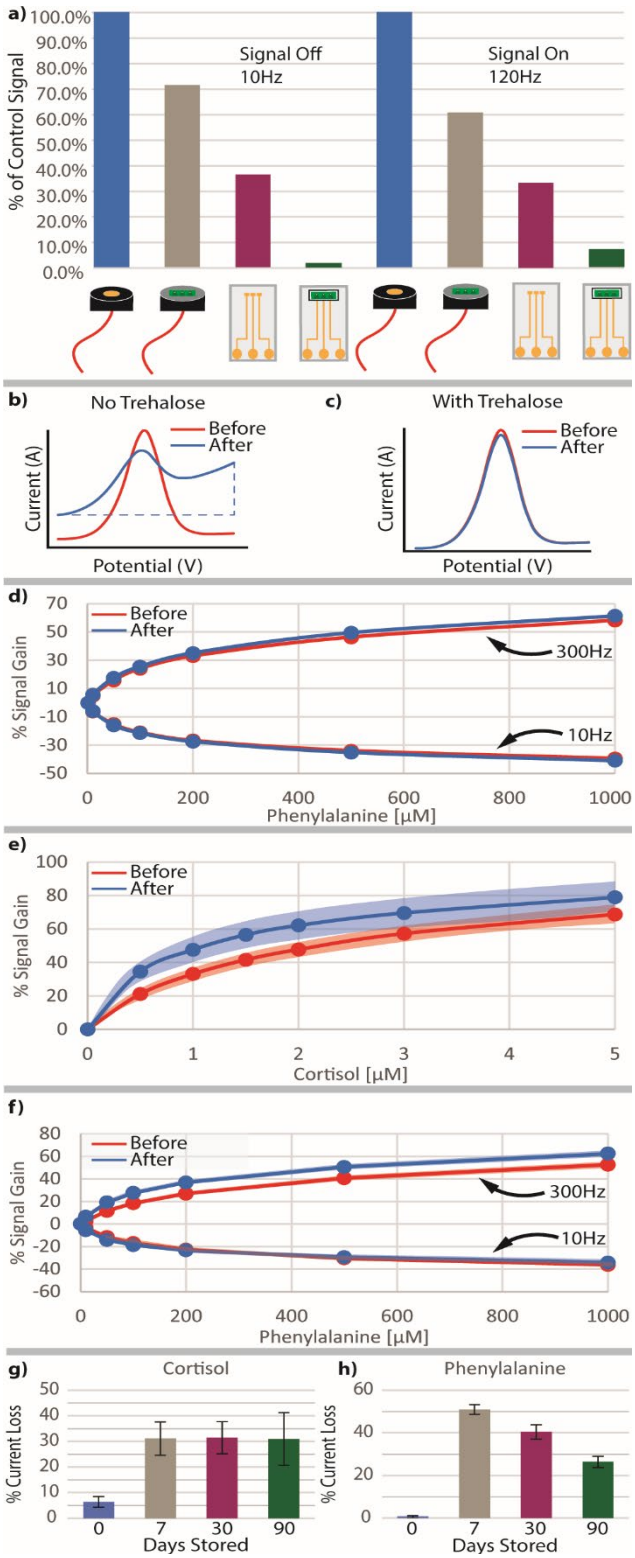

Figure 4 – Comparison of device design and storage effects on sensor functionality. a. Relative signal strength of various sensor fabrication methods and assemblies compared to a bare disc electrode for a phenylalanine sensor measured at 10 and 120 Hz. **b.** Visualization of destructive vacuum effects on unprotected EAB sensors via effect on the square wave voltammogram. **c.** Comparison of square wave voltammograms after vacuum with 10% w/w trehalose preservation on phenylalanine sensors and **d.** a titration of these same sensors. **e.** Titration of cortisol and **f**. phenylalanine sensors after 90-days of dry, trehalose storage with shaded error ranges. **g.** Bulk signal loss after 0, 7, 30, and 90 days of storage for cortisol and **h**. phenylalanine sensors.

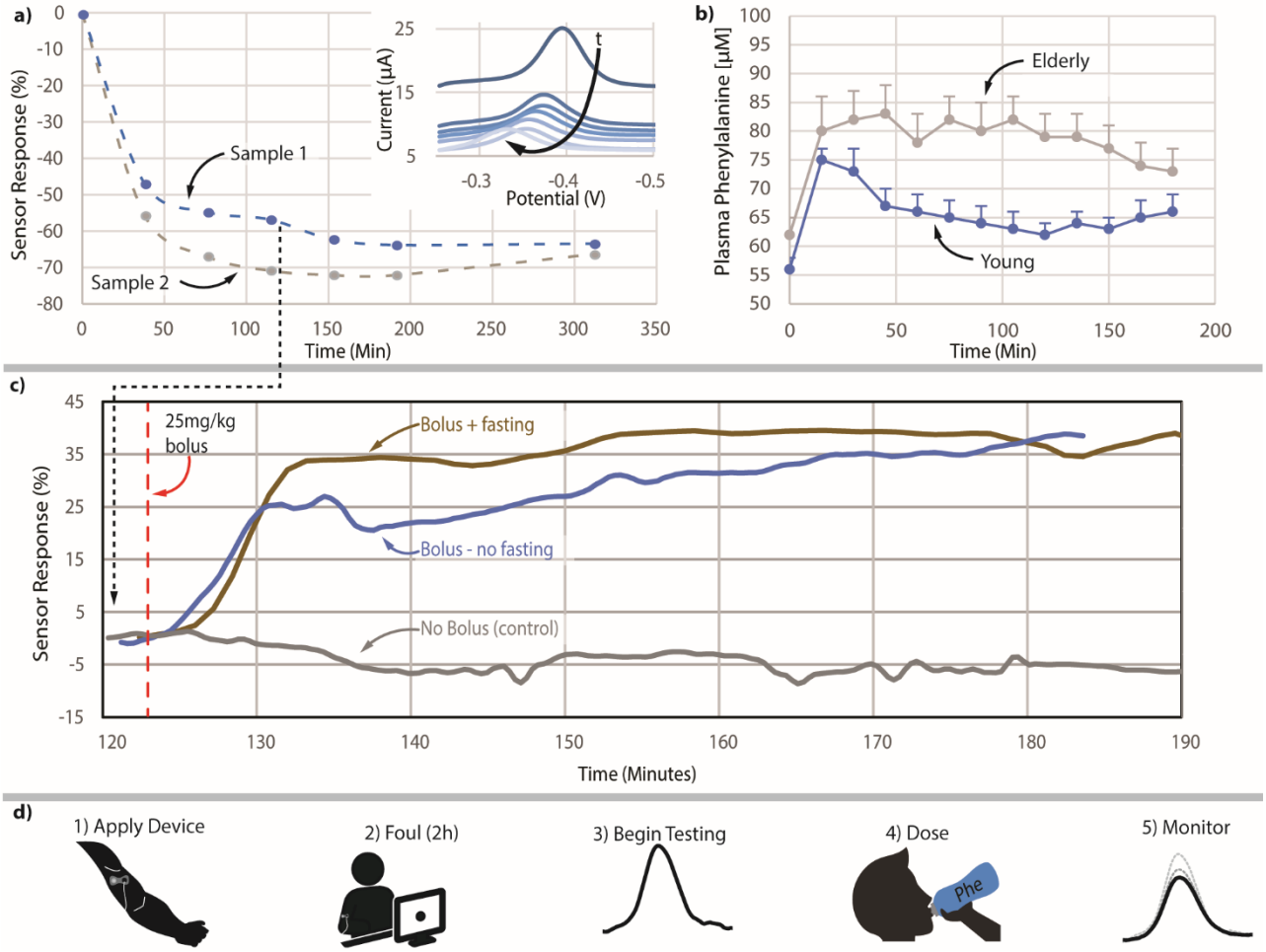

Figure 5 – On-body device testing. a. On-body signal response of planar electrodes worn to assess sensor warmup (fouling) effects with inset graph of voltammograms showing square wave response over 5 h. **b.** Data adapted from Koopman et al.[20] showing blood phenylalanine levels after an oral bolus for comparison with **c.** On-body sensor response to phenylalanine dosage. **d.** Schematic of testing workflow.

draw-based studies reported a rapid increase in plasma phenylalanine with heightened levels sustained thereafter[20] (figure 5b). We do, however, observe a mild drift in signal after phenylalanine uptake (>30 min post ingestion)), presumably due to sensor degradation (figure 5c). This degradation could be potentially resolvable using our recently reported methods to improve sensor longevity to greater than one week[21].

Throughout this work we made significant compromises to achieve high-frequency, on-body dose-response measurements. For example, when challenged free in solution, our phenylalanine aptamer sensor achieves greater signal gain and peak currents at higher square-wave frequencies (> 60 Hz; SI figure 2). However, at frequencies above 120 Hz the peak current of our microneedle devices is either indistinguishable from noise or does not respond to challenge with phenylalanine. Because of this, which could be due to the capacitive-resistance charging effects present when including the epidermis into the electrical circuit, we collected our on-body data using a 10 Hz square-wave frequency. By limiting our measurements to this single frequency we are unable to determine absolute phenylalanine concentrations because we cannot employ calibration free measurement techniques[22]. Ultimately, we could mitigate this effect by moving the counter electrode onto the backside of the microneedle substrate to remove the epidermis from the device circuit.

Discussion

Herein, we demonstrate the first continuous measurements of affinity-based aptamer sensors in human subjects. We achieved this by coupling ex vivo sensors to ISF via minimally-invasive, fluid-filled microneedles. In parallel, we report several advances in the manufacturing and storage of such devices. Although we faced multiple limitations in the design of this device, the results presented here demonstrates the feasibility of electrochemical aptamer-based sensors as a continuous sensing modality able to work directly on the human body. To move beyond feasibility studies, continued research into the circuitry through the microneedles and dermis to improve the range of square-wave frequencies that can be employed to interrogate this and similar aptamer sensor devices, which could unlock the ability to correct for sensor drift through kinetic differential measurement[22,23] and to achieve quantitative in vivo measurements.

While the work presented here represents a milestone in our efforts to move beyond just continuous glucose monitoring,

we believe the potential value of the specific approach used herein deserves additional comment. At this time, it is our opinion that the device presented here has strong utility as an academic research tool because: (1) the device presented leverages use of simple disc electrodes, which are widely utilized for in-vitro electrochemical sensor development; (2) leverages use of commercial FDA-approved microneedles, thus easing development burden for other groups desiring to move to human testing; and (3) places the sensors ex-vivo such that any materials that are not-biocompatible simply need be locally immobilized, easing development burden regarding safe insertion into and removal from human subjects. This said, however, it is difficult to speculate on the potential clinical utility of this microneedle device. As such, the technology described here may speed the ability in which others are able to pursue human testing of continuous biosensors.

Methods

Electrode Fabrication

We employed two electrode formats, thin-film gold or gold disc electrodes, which we created using the following workflow. Disc electrodes were constructed by cutting 2 mm diameter gold working electrodes (CH Instruments, Austin, TX) to ~4 mm in thickness. After cutting, a working electrode wire was connected to the newly exposed gold surface with conductive, AgCl epoxy 8331D (MG Chemicals, British Columbia, Canada) and insulated with epoxy to passivate the exposed wire. We fabricated our thin-film gold electrodes as follows. Borosilicate glass was prepared for deposition by cleaning in piranha (5:1 H_2SO_4:H_2O_2) followed by e-beam deposition of a 10 nM titanium layer for adhesion followed by a 100 nM gold layer. We patterned thin-film electrode via a wet etch process using AZ1518 positive photoresist with AZ400k developer (MicroChemicals, Ulm, Germany). Then we etched gold using aqua regia (3:1 HCl:HNO_3) followed by etching of titanium with a hydrofluoric acid (HF) solution (1:1:40 HF:H_2O_2:H_2O). Residual photoresist was removed by rinsing with acetone. The CAD drawings for these custom electrodes are provided with the online supplemental material.

Sensor Preparation

Thin-film and disc electrodes were functionalized into aptamer sensors using similar processes. Specifically, our disc electrodes required an additional cleaning step before functionalization with aptamer in which we mechanically polished them using micro cloths soaked in 0.3 µm alumina slurry (eDAQ, Colorado Springs, CO). Both electrode types were then electrochemically cleaned using cyclic voltammetry in base followed by acid similar to prior work[24]. After cleaning, we incubated the electrodes in 400 nM aptamer (sequences provided in table 1) for 1 h at room temperature followed by overnight incubation in 5 mM 6-mercapto-1-hexanol (mercaptohexanol) at 4°C. For in-vivo testing the aptamer sensors were disinfected using CIDEX solution as reported previously[25].

Table 1- Aptamer sequences.

Target	Sequence (5' – 3')
Phenylalanine	SH-$(CH_2)_6$-CGACC-GCGTT-TCCCA-AGAAA-GCAAG-TATTG-GTTGG-TCG-MB
Cortisol	MB-GGA-CGA-CGC-CAG-AAG-TTT-ACG-AGG-ATA-TGG-TAA-CAT-AGT-CGT-$(CH_2)_6$-SH
Vancomycin	SH-$(CH_2)_6$-CGAGG-GTACC-GCAAT-AGTAC-TTATT-GTTCG-CCTAT-TGTGG-GTCGG-MB

[Footnote] MB stands for the redox reporter methylene blue and 'SH-$(CH_2)_6$' is the hexathiol attachment used to attach the aptamer sensor to gold electrodes.

Aptamer Protection and Storage Testing

Disc electrodes were tested in 1x phosphate buffer saline (PBS), pH 7.4 with a short titration of target analyte using square wave voltammetry (SWV) at 120 Hz for cortisol sensors and 10 Hz and 300 Hz for phenylalanine sensors with a CH Instruments 620E potentiostat (CH Instruments, Austin, TX). Testing was completed using the following workflow: (1) we prepared sensors as normal, (2) then we collected sensor data while titrating target (3) we washed sensors in buffer solution (4) we dried sensors under vacuum with 10%w/w trehalose in PBS solution (5) we placed sensors into dry nitrogen storage (6) we rehydrated sensors and repeat the data collection of step 2. To store sensors, we deposited trehalose solution onto the sensor surface then applied -25 inHg vacuum until trehalose fully dried (~1 h). After storage, sensors were rehydrated in PBS and retested under the same conditions as before storage.

Microneedle Device Assembly

Electrodes were assembled into microneedle devices using 3x1 arrays of 600-micron tall silicon microneedles (Nanopass Technologies, Ness Ziona, Israel) that are FDA approved for human use with their existing indication being for injection of drugs into the skin. First, we laser cut adhesive spacers (Universal Laser Systems, Scottsdale, AZ) from double-sided, 90 µm thick microfluidic tape (9965, 3M, Saint Paul, MN) to attach the microneedles to the aptamer sensor substrate and to define the volume of the sensing cavity (Figure 2). Prior to attaching the microneedles onto the sensor substrates, we coated the sensor electrodes with 10% w/w trehalose solution and dried them under vacuum. Then, we added auto-clave sterilized microneedle substrate onto the adhesive spacer window. For thin-film electrodes polyimide tape was used to electrically insulate any exposed gold. At this point these devices may be shelf-stored in a dry, nitrogen environment for 90 days or more. Prior to human subject testing the microneedles and sensing cavity were wetted with sterile PBS solution by placing the sensors under -25 inHg vacuum for 15 min and then submerging them in PBS while still under vacuum. The vacuum was then released to fill the sensors and microneedles. All devices were tested immediately after filling. CAD files with dimensions for the parts described below are included in the online supplemental files.

Simulating Device Lag Time

Device lag time simulations were run in COMSOL to estimate the time required for an analyte in the dermis to reach and equilibrate in concentration inside the sensor cavity. As shown in figure 4b, a simple geometry was employed to track analyte partitioning from the dermis through the needle to the furthest point in the sensing cavity. Geometry was defined to match the thin-film sensors as follows: a 600 µm needle lumen with a 30 µm radius, a 90 µm tall sensor cavity with a 60 µm length to the furthest point, and a vastly larger dermis at 5x5 mm. Stabilized Convection-Diffusion Kinetics were applied to a 2D axisymmetric model. Parametric sweeps were used to test various diffusivities of analytes: 7.8E-10m^2/s for phenylalanine[26], 6.7E-10 m^2/s for glucose[27], 2.8E-10 m^2/s for vancomycin[28], and 2.7E-11 m^2/s for Interluekin-6 (IL-6)[29]. We note that these simulations do not consider the population of aptamers on the sensor surface which for very low (picomolar) concentrations of analytes can increase lag time. Given the small volumes in the microneedle device, the amount of analyte bound to the aptamers (which are at ~10^{11}-10^{13} aptamers per cm^2)[30] can substantially reduce the free target concentration.

Device Testing

We report both *in-vitro* and *in-vivo* results completed with the following considerations. We tested sensors *In-vitro* using either PBS or raw bovine serum, the latter containing unknown concentrations of endogenous cortisol and phenylalanine. A potentiostat was used to collect square wave voltammetry data periodically while analyte was added or solution outside of the sensor was replaced to increase or lower concentration (Figure 3c-g). Human subjects testing was completed under protocols approved by the University of Cincinnati's Institutional Review Board. Phenylalanine sensing devices were built, inserted into the dermis, and secured into place with medical tape (1776, 3M, Saint Paul, MN). Sensor longevity tests were performed for up to 6 h to track sensor fouling and stability while participants completed light daily tasks, returning for sensor measurements periodically. In dose-response tests, sensors placed on-body fouled and equilibrated with endogenous phenylalanine for 2 h before continuous measurement began. After a short data collection period, participants received a 25 mg/kg phenylalanine dosed orally (figure 5d). On-body square wave parameters tested were as follows: 35 mV amplitude pulse, step frequencies ranging from 10-60 Hz, and a 2 mV step potential.

Author Contributions

Mark Friedel: Conceptualization, Formal Analysis, Investigation, Methodology, Supervision, Validation, Visualization, Writing - Original Draft, Writing - Review & Editing. **Benjamin Werbovetz:** Investigation, Validation, Formal Analysis. **Amy Drexelius:** Investigation, Validation. **Kevin W. Plaxco:** Funding Acquisition, Writing - Review & Editing. **Jason Heikenfeld:** Conceptualization, Funding Acquisition, Methodology, Supervision, Writing - Review & Editing

Conflicts of interest

Author Heikenfeld is a co-founder of Kilele Health Inc. which is pursuing commercialization of continuous wearable monitoring of analytes in ISF.

Acknowledgements

The authors at the University of Cincinnati acknowledge support from the U.S. Office of Naval Research Award #N00014-20-1-2764), from a National Science Foundation ECCS Award #2025720, from the National Science Foundation CBET Award #2125056, and from U.S. Air Force Office of Scientific Research USAF Contract No. FA9550-20-1-0117.

Notes and references

1 J. Heikenfeld, A. Jajack, B. Feldman, S. W. Granger, S. Gaitonde, G. Begtrup and B. A. Katchman, Accessing analytes in biofluids for peripheral biochemical monitoring, *Nature Biotechnology*, , DOI:10.1038/s41587-019-0040-3.

2 M. J. Tierney, Y. Jayalakshmi, N. A. Parris, M. P. Reidy, C. Uhegbu and P. Vijayakumar, Design of a Biosensor for Continual, Transdermal Glucose Monitoring, *Clinical Chemistry*, 1999, **45**, 1681–1683.

3 B. Q. Tran, P. R. Miller, R. M. Taylor, G. Boyd, P. M. Mach, C. N. Rosenzweig, J. T. Baca, R. Polsky and T. Glaros, Proteomic Characterization of Dermal Interstitial Fluid Extracted Using a Novel Microneedle-Assisted Technique, *J Proteome Res*, 2018, **17**, 479–485.

4 R. M. Taylor, P. R. Miller, P. Ebrahimi, R. Polsky and J. T. Baca, Minimally-invasive, microneedle-array extraction of interstitial fluid for comprehensive biomedical applications: transcriptomics, proteomics, metabolomics, exosome research, and biomarker identification, *Lab Anim*, 2018, **52**, 526–530.

5 P. R. Miller, R. M. Taylor, B. Q. Tran, G. Boyd, T. Glaros, V. H. Chavez, R. Krishnakumar, A. Sinha, K. Poorey, K. P. Williams, S. S. Branda, J. T. Baca and R. Polsky, Extraction and biomolecular analysis of dermal interstitial fluid collected with hollow microneedles, *Communications Biology*, 2018, **1**, 1–11.

6 M. Friedel, I. A. P. Thompson, G. Kasting, R. Polsky, D. Cunningham, H. T. Soh and J. Heikenfeld, Opportunities and challenges in the diagnostic utility of dermal interstitial fluid, *Nat. Biomed. Eng*, 2023, 1–15.

7 N. Arroyo-Currás, P. Dauphin-Ducharme, K. Scida and J. L. Chávez, From the beaker to the body: translational challenges for electrochemical, aptamer-based sensors, *Anal. Methods*, 2020, **12**, 1288–1310.

8 A. Ruscito and M. C. DeRosa, Small-Molecule Binding Aptamers: Selection Strategies, Characterization, and Applications, *Front Chem*, , DOI:10.3389/fchem.2016.00014.

9 L. Gold, D. Ayers, J. Bertino, C. Bock, A. Bock, E. Brody, J. Carter, V. Cunningham, A. Dalby, B. Eaton, T. Fitzwater, D. Flather, A. Forbes, T. Foreman, C. Fowler, B. Gawande, M. Goss, M. Gunn, S. Gupta, D. Halladay, J. Heil, J. Heilig, B. Hicke, G. Husar, N. Janjic, T. Jarvis, S. Jennings, E. Katilius, T. Keeney, N. Kim, T. Kaske, T. Koch, S. Kraemer, L. Kroiss, N. Le, D. Levine, W. Lindsey, B. Lollo, W. Mayfield, M. Mehan, R. Mehler, M. Nelson, S. Nelson, D. Nieuwlandt, M. Nikrad, U. Ochsner, R. Ostroff, M. Otis, T. Parker, S. Pietrasiewicz, D. Resnicow, J. Rohloff, G.

Sanders, S. Sattin, D. Schneider, B. Singer, M. Stanton, A. Sterkel, A. Stewart, S. Stratford, J. Vaught, M. Vrkljan, J. Walker, M. Watrobka, S. Waugh, A. Weiss, S. Wilcox, A. Wolfson, S. Wolk, C. Zhang and D. Zichi, Aptamer-based multiplexed proteomic technology for biomarker discovery, *Nat Prec*, 2010, 1–1.

10 A. Idili, J. Gerson, T. Kippin and K. W. Plaxco, Seconds-Resolved, In Situ Measurements of Plasma Phenylalanine Disposition Kinetics in Living Rats, *Anal. Chem.*, , DOI:10.1021/acs.analchem.0c05024.

11 J.-W. Seo, K. Fu, S. Correa, M. Eisenstein, E. A. Appel and H. T. Soh, *Real-time monitoring of drug pharmacokinetics within tumor tissue in live animals*, 2021.

12 F. Tehrani, H. Teymourian, B. Wuerstle, J. Kavner, R. Patel, A. Furmidge, R. Aghavali, H. Hosseini-Toudeshki, C. Brown, F. Zhang, K. Mahato, Z. Li, A. Barfidokht, L. Yin, P. Warren, N. Huang, Z. Patel, P. P. Mercier and J. Wang, An integrated wearable microneedle array for the continuous monitoring of multiple biomarkers in interstitial fluid, *Nat. Biomed. Eng*, 2022, 1–11.

13 S. Lin, X. Cheng, J. Zhu, B. Wang, D. Jelinek, Y. Zhao, T.-Y. Wu, A. Horrillo, J. Tan, J. Yeung, W. Yan, S. Forman, H. A. Coller, C. Milla and S. Emaminejad, Wearable microneedle-based electrochemical aptamer biosensing for precision dosing of drugs with narrow therapeutic windows, *Science Advances*, 2022, **8**, eabq4539.

14 Y. Yuan, M. DeBrosse, M. Brothers, S. Kim, A. Sereda, N. V. Ivanov, S. Hussain and J. Heikenfeld, Oil-Membrane Protection of Electrochemical Sensors for Fouling- and pH-Insensitive Detection of Lipophilic Analytes, *ACS Appl. Mater. Interfaces*, 2021, **13**, 53553–53563.

15 A. Jajack, I. Stamper, E. Gomez, M. Brothers, G. Begtrup and J. Heikenfeld, Continuous, quantifiable, and simple osmotic preconcentration and sensing within microfluidic devices, *PLOS ONE*, 2019, **14**, e0210286.

16 A. McHenry, M. Friedel and J. Heikenfeld, Voltammetry Peak Tracking for Longer-Lasting and Reference-Electrode-Free Electrochemical Biosensors, *Biosensors*, 2022, **12**, 782.

17 A. Jina, M. J. Tierney, J. A. Tamada, S. McGill, S. Desai, B. Chua, A. Chang and M. Christiansen, Design, development, and evaluation of a novel microneedle array-based continuous glucose monitor, *J Diabetes Sci Technol*, 2014, **8**, 483–487.

18 N. V. Ivanova and M. L. Kuzmina, Protocols for dry DNA storage and shipment at room temperature, *Mol Ecol Resour*, 2013, **13**, 890–898.

19 N. Arroyo-Currás, K. Scida, K. L. Ploense, T. E. Kippin and K. W. Plaxco, High Surface Area Electrodes Generated via Electrochemical Roughening Improve the Signaling of Electrochemical Aptamer-Based Biosensors, *Anal. Chem.*, 2017, **89**, 12185–12191.

20 R. Koopman, N. Crombach, A. P. Gijsen, S. Walrand, J. Fauquant, A. K. Kies, S. Lemosquet, W. H. Saris, Y. Boirie and L. J. van Loon, Ingestion of a protein hydrolysate is accompanied by an accelerated in vivo digestion and absorption rate when compared with its intact protein, *The American Journal of Clinical Nutrition*, 2009, **90**, 106–115.

21 Z. Watkins, A. Karajic, T. Young, R. White and J. Heikenfeld, Week-long operation of electrochemical aptamer sensors: New insights into self-assembled monolayer degradation mechanisms and solutions for stability in biofluid at body temperature.

22 H. Li, P. Dauphin-Ducharme, G. Ortega and K. W. Plaxco, Calibration-Free Electrochemical Biosensors Supporting Accurate Molecular Measurements Directly in Undiluted Whole Blood, *J. Am. Chem. Soc.*, 2017, **139**, 11207–11213.

23 A. Idili, C. Parolo, G. Ortega and K. W. Plaxco, Calibration-Free Measurement of Phenylalanine Levels in the Blood Using an Electrochemical Aptamer-Based Sensor Suitable for Point-of-Care Applications, *ACS Sens*, 2019, **4**, 3227–3233.

24 Y. Xiao, R. Y. Lai and K. W. Plaxco, Preparation of electrode-immobilized, redox-modified oligonucleotides for electrochemical DNA and aptamer-based sensing, *Nature Protocols*, 2007, **2**, 2875–2880.

25 J. Chung, L. Sepunaru and K. W. Plaxco, On the Disinfection of Electrochemical Aptamer-Based Sensors, *ECS Sens. Plus*, 2022, **1**, 011604.

26 T. Umecky, K. Ehara, S. Omori, T. Kuga, K. Yui and T. Funazukuri, Binary Diffusion Coefficients of Aqueous Phenylalanine, Tyrosine Isomers, and Aminobutyric Acids at Infinitesimal Concentration and Temperatures from (293.2 to 333.2) K, *J. Chem. Eng. Data*, 2013, **58**, 1909–1917.

27 M. Kreft, M. Lukšič, T. M. Zorec, M. Prebil and R. Zorec, Diffusion of D-glucose measured in the cytosol of a single astrocyte, *Cell Mol Life Sci*, 2013, **70**, 1483–1492.

28 Q. Zhu, X. Gao, M. D. Brown, F. Eismont and W. Gu, Transport of Vancomycin and Cefepime Into Human Intervertebral Discs: Quantitative Analyses, *Spine*, 2019, **44**, E992.

29 G. J. Goodhill, Diffusion in Axon Guidance, *European Journal of Neuroscience*, 1997, **9**, 1414–1421.

30 R. J. White, N. Phares, A. A. Lubin, Y. Xiao and K. W. Plaxco, Optimization of electrochemical aptamer-based sensors via optimization of probe packing density and surface chemistry, *Langmuir*, 2008, **24**, 10513–10518.